

## **Formation and Evolution of Binary Millisecond Pulsars with Helium White Dwarf Companions**

Lorne A. Nelson

*Physics Department, Bishop's University, 40 College St., Lennoxville,  
QC Canada J1M 1Z7*

### **Abstract.**

Our current understanding of the formation and evolution of wide galactic binary millisecond pulsars (BMSPs) containing helium white dwarf (HeWD) companions is reviewed. The detailed evolution of progenitor systems containing (sub)giants that ultimately become HeWDs as a result of transferring most of their mass to their (accreting) neutron star companions is investigated. Given the recent determinations of reasonably precise values of the masses and effective temperatures of some HeWDs, it has become possible to test the theoretical models. Although there is good agreement between the model predictions and the observations, there are a number of discrepancies between the characteristic ages of pulsars (inferred from their spin-down times) compared to the cooling times of the HeWDs. The reasons for the discrepancies and possible resolutions are briefly discussed. The importance of the bifurcation limit is also emphasized and the conditions leading to the formation and evolution of ultracompact systems is examined. Finally new developments concerning the evolution of the eclipsing BMSP J1740-5340 and the formation of ‘red stragglers’ in globular clusters are discussed.

### **1. Introduction**

Binary MilliSecond Pulsars (BMSPs) provide us with one of the best means to test our understanding of the many diverse physical processes that occur in close interacting binaries. Of particular interest are the millisecond or ‘recycled’ pulsars. The majority of these pulsars are found in binary systems and this affirms the hypothesis that the short rotational periods are caused by the accretion of matter from a companion that had previously overfilled its Roche lobe. Furthermore it is clear that only a neutron star with a small magnetic field ( $\sim 10^8 - 10^9$  G) can be spun up to ultrashort rotational periods of  $\sim 1$  msec (for a review, see Bhattacharya & van den Heuvel 1991; Phinney & Kulkarni 1994).

It took nearly 20 years from the time of the discovery of the first MSP (PSR J1937+21; Backer et al. 1982) before an accreting MSP was observed (SAX J1808-37; Wijnands & van der Klis 1998). Since that time, four more accreting MSPs have been detected. Their discovery provides strong evidence that the “recycling hypothesis” is correct and underscores the idea that low- and intermediate-mass X-ray binaries are the progenitors of MSPs.

The evolution of BMSPs located in globular clusters should be distinguished from those in the galactic disk because of the potentially very different formation scenarios. In the cores of globular clusters there is a reasonably high probability of exchange interactions occurring wherein an ordinary star in a close binary is exchanged for a neutron star (NS). Because dynamics plays such an important role in the evolution of globular cluster sources, I will only review our understanding of the formation and evolution of galactic systems (and in particular those BMSPs containing helium-rich white dwarf companions [HeWDs]).

There are approximately 35 BMSPs with nearly circular orbits ( $e \lesssim 0.01$ ) that are in orbit with low-mass companions ( $0.1 \lesssim M/M_{\odot} \lesssim 0.5$ ) in the disk of our galaxy (for a compilation see the ATNF Pulsar Catalogue). Their orbital periods ( $P_{orb}$ ) range from about 6 hours to more than 1000 days and there appears to be a statistically significant gap in the orbital-period distribution between 23 and 56 days (Taam, King, & Ritter 2000; Nelson & Dubeau 2004). About 20 of the companions of the MSPs have been identified optically and of those approximately 10 have had their spectra analyzed (van Kerkwijk 2004). The optical analysis of the properties of the companions plays a crucial role in constraining the theoretical models (see §3). These measurements allow us to carry out very important consistency checks of the cooling times of the (degenerate) companions against the characteristic ages of the pulsars as inferred from their spin-down derivatives.

## 2. Formation and Evolution of BMSPs

The presently observed properties of BMSPs depend critically on the evolutionary pathway that led to their formation. These pathways are characterized primarily by: (1) the way in which the NS was formed; and (2) the mass of the donor and the orbital separation after the birth of the neutron star. With respect to the first issue, it is generally believed that the more massive star in the primordial binary undergoes a phase of common envelope (CE) evolution wherein the companion star spirals in towards the center of the massive star ( $\sim 10 - 30M_{\odot}$ ) ejecting most of its envelope and leaving behind a He-burning core. The NS is subsequently born after the explosion of the He star. If the binary is not disrupted but remains in a relatively close orbit, it may be possible for the donor to transfer mass to the NS producing a bright X-ray binary that may ultimately evolve to become a BMSP (for more details see Willems & Kolb 2002; Pfahl, Rappaport, & Podsiadlowski 2003, and references therein). Another channel that could lead to the birth of a NS results from the accretion-induced collapse (AIC) of an ONeMg white dwarf (see, e.g., Bitzaraki et al. 2003). For this scenario to be viable the progenitor of the ONeMg WD must lie in a relatively narrow range ( $\sim 8 - 9M_{\odot}$ ). With respect to the second issue, the mass of the donor and its separation from the neutron star will dictate the subsequent evolution. If the binary is sufficiently tightly bound after circularization then it may be possible for mass transfer to commence while the donor is still on the main sequence (Case A mass transfer). Alternatively, if the donor must expand significantly to fill its Roche lobe (e.g., Case B or Case C mass transfer) and if it avoids a dynamical instability, then it is likely to form a BMSP consisting of a degenerate companion and a recycled pulsar.

The relative probabilities of the various evolutionary channels can be calculated using binary population synthesis (BPS) techniques. BPS analyses have been quite successful in explaining the ensemble properties of cataclysmic variables (see, e.g., Howell, Nelson & Rappaport 2001, and references therein). More recent studies have addressed the issue of the formation and evolution of compact binaries containing neutron stars. Because of the large number of uncertain parameters that must be specified in order to carry out such studies (e.g., initial masses of the primordial binary components, SN kick velocities, and the efficiency of accretion onto the NS) and the additional complication of simulating the formation of the neutron star, it has been difficult to formulate definitive conclusions. The results of BPS studies should be able to account for all of the features associated with the orbital period distribution of BMSPs and yield the correct number of X-ray binaries observed at the present epoch. This has proved to be particularly challenging both in terms of explaining the number of BMSPs observed to have  $P_{orb}$ s of less than 10 days and reproducing the observed numbers of X-ray binaries (the ‘birthrate problem’).

While there are many problems to be addressed, the evolutionary pathway that the donor follows after it starts to transfer mass to the NS is reasonably well understood. Generally speaking, the nascent neutron-star binary can either evolve to large values of  $P_{orb}$  (diverging systems) or to small ones (converging). The *bifurcation limit* delineates these two very distinct regimes (Pylyser & Savonije 1988). Systems evolving above the bifurcation limit will usually produce widely separated, nearly circular BMSPs while those below the limit are observed almost exclusively as low-mass X-ray binaries (LMXBs) that are evolving towards very short orbital periods ( $\lesssim 1$  hour). The location of the bifurcation limit is largely governed by the relative magnitudes of the mass-loss timescale  $[\tau_{\dot{m}}]$  of the donor and its nuclear evolution timescale  $[\tau_{nuc}]$ . The mass-loss timescale itself depends on the properties of both the donor and the binary, and on the mode of angular momentum dissipation. The detailed evolution and ultimate fate of the binary system also depends on other physical timescales such as the thermal timescale of the donor or its envelope (i.e.,  $\tau_{KH}$  or  $\tau_{env}$ ). Typically donors for which  $\tau_{nuc} \ll \tau_{\dot{m}}$  have sufficiently short nuclear timescales that they can enter the Hertzsprung gap or become giants before losing too much mass (i.e., diverging systems). For systems for which  $\tau_{nuc} \gg \tau_{\dot{m}}$ , the evolution is governed largely by orbital angular momentum losses due to gravitational radiation, magnetic stellar wind (MSW) braking, and systemic mass loss. These systems typically evolve from orbital periods of less than one day to an orbital period minimum (typically about 80 minutes) and then slowly evolve back to longer periods. If the donor is close to the bifurcation limit it can become very H-depleted and this tends to make it much smaller than its H-rich counterpart. In extreme cases it is possible for the donor to become so small that the minimum value of  $P_{orb}$  is reduced to  $\sim 8$  minutes (see, e.g., Nelson & Rappaport 2003, [NR]).

Binaries evolving above the bifurcation limit give rise to two distinctly different types of companions. (1) LMBPs have low-mass companions ( $0.14 \lesssim M/M_{\odot} \lesssim 0.46$ ) that are composed of He-rich cores and very low-mass, hydrogen-rich envelopes ( $\lesssim 10^{-2} M_{\odot}$ ). The upper and lower limits on the mass range can be understood as follows: the upper limit corresponds approximately to

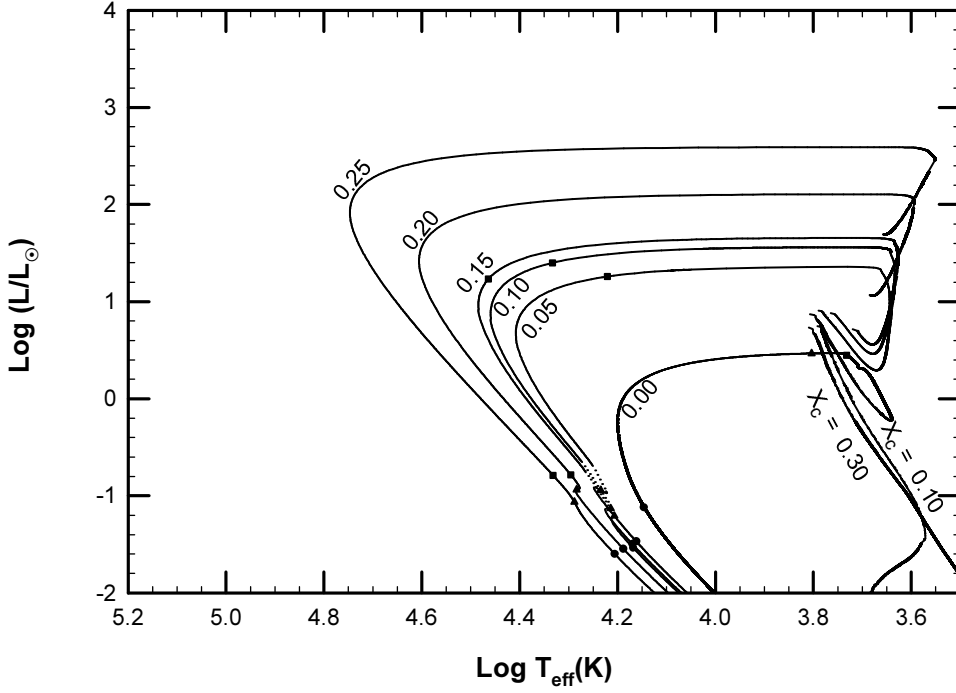


Figure 1. Evolutionary tracks of donors with initial masses of  $1.5M_{\odot}$  ( $Z = 0.02$ ). The numbers adjacent to each track correspond to the helium core mass (in units of  $M_{\odot}$ ) at the onset of mass transfer. Those labeled by  $X_c$  denote the initial values of the central hydrogen content (no cores had formed at that point). The dotted lines denote the location of the beginning and ending of vigorous shell flashes. The age of the donor after its detachment from the Roche lobe (after turning off the RGB) is denoted by squares ( $10^7$  yr), triangles ( $10^8$  yr), and dots ( $10^9$  yr).

the maximum mass that the He-rich core of a star ascending the red giant branch can have before undergoing He ignition. The lower limit arises because of the Chandrasekhar-Schönberg limit which specifies the maximum mass that an isothermal He core can have before it collapses ( $\sim 10-15\%$  of the star's mass). (2) The IMBP's typically have more massive companions ( $0.3 \lesssim M/M_{\odot} \lesssim 0.9$ ) that are composed of a C-O core and a thick He-rich envelope. The lower mass limit for this class of donors is governed by the minimum core-mass that a star can have in order to burn He non-degenerately.

If the initial mass of the donor is between  $\sim 1$  and  $2M_{\odot}$  when it first fills its Roche lobe (and assuming that it is sufficiently evolved to lie above the bifurcation limit), the binary will evolve to produce a HeWD in a wide orbit with a MSP (LMBP). If the donor has started to burn He in its core, it is possible for the binary to evolve to very long orbit periods. Tauris, van den Heuvel,

& Savonije (2000) and Podsiadlowski, Rappaport, & Pfahl (2002, [PRP]) have shown that if the convective envelope of donors in the mass range of  $\sim 2$  to  $5M_{\odot}$  is not too deep, it is possible the system to avoid a dynamical instability and produce either a HeWD or C-O WD companion in a relatively short-period orbit of between about 1 to 10 days (see figure 4 of Tauris et al. 2000). For the remainder of this review, however, I will focus on the evolution of LMBPs containing HeWDs and show why the study of these particular systems gives us special insights into the evolution of BMSPs as a whole.

### 3. Evolution of LMBPs

It has long been recognized that if  $\tau_{nuc} \ll \tau_m$ , then a low-mass donor will evolve through the subgiant phase and form a helium core. As the donor ascends the RGB (while losing mass) the H-burning shell continues to burn outwards thereby increasing the mass of the core. Eventually the hydrogen-rich envelope surrounding the helium core becomes so diffuse that it cannot be supported and the subsequent collapse leaves behind a detached (cooling) remnant in orbit with its spun-up NS companion. Since the properties of red giants are dictated primarily by their core masses,  $m_c$ , and not by the mass of the stars themselves or by the mass-transfer rate,  $\dot{M}_2$ , it is possible to calculate a semi-analytic relationship between the final orbital periods of BMSPs and the remnant (core) masses (see, e.g., Rappaport et al. 1995, and references therein).

The parameter space needed to fully investigate the evolution of this type of binary system is inherently five dimensional. The vector of parameter space contains the following elements: (i) the initial mass of the donor ( $M_{2,o}$ ); (ii) the initial mass of the accretor ( $M_{1,o}$ ); (iii) the initial chemical profile of the interior of the donor star (which can be correlated with its initial  $P_{orb,o}$ ); (iv) the metallicity of the donor ( $Z$ ); and, (v) the mode of orbital angular momentum loss that drives mass transfer and the degree to which systemic mass-loss occurs. Nelson, Dubeau, & MacCannell (2004, [NDM]) calculated a grid of approximately 200 evolutionary sequences corresponding to initial donor masses of  $M_{2,o} = 1, 1.5,$  and  $2M_{\odot}$ . It was assumed that gravitational radiation and MSW braking (Rappaport, Verbunt, & Joss 1984 parameterization with  $\gamma = 3$ ) were responsible for orbital angular momentum losses. As a limiting case, mass transfer was assumed to be completely non-conservative (i.e.,  $\beta \equiv \dot{M}_{NS}/|\dot{M}_2| = 0$ ), and it was further assumed that the matter lost from the system was lost rapidly and isotropically thereby carrying away a specific angular momentum equal to that of the NS accretor (i.e., fast Jeans' mode). In reality we know that MSPs should be more massive than they were at birth (typically MSPs need to accrete  $\lesssim 0.1M_{\odot}$  to be spun up). While there is some statistical evidence to support this claim, the most precisely determined MSP masses are not much larger than the canonical value of  $1.4M_{\odot}$ ; the observationally inferred values are: (i)  $1.58 \pm 0.18M_{\odot}$  for PSR J0437+4715 (van Straten et al. 2001); and, (ii)  $1.57^{+0.12}_{-0.11}M_{\odot}$  for PSR B1855+09 (Nice, Splaver, & Stairs 2003). These results would certainly seem to imply that accretion is highly inefficient (i.e.,  $\beta \ll 1$ ). A previous theoretical study of the evolution of LMXBs by Tauris & Savonije (1999) led them to conclude that a substantial fraction of transferred material is ejected even when the neutron stars are accreting at sub-Eddington levels (they suggest disk instabilities or

the propellor effect as the cause). NDM also calculated the evolution of a large number of tracks under the constraint of purely conservative mass transfer (i.e.,  $\beta = 1$ ) and concluded that the evolution of systems that are not too close to the bifurcation limit is not greatly affected. The effects of X-ray irradiation on the donor were not included and no clear picture has yet to emerge concerning its importance.

### 3.1. Results

Evolutionary tracks of  $1.5M_{\odot}$  donors with a solar metallicity ( $Z = 0.02$ ) are shown in Figure 1. The mass of the NSs for all cases is  $1.4M_{\odot}$ . The most striking features are: (i) the very distinct bifurcation in the evolutionary tracks (above the limit donors ascend the RGB and produce degenerate remnants while below the limit donors evolve to ever decreasing luminosities); and, (ii) the occurrence of vigorous hydrogen shell flashes while the donors are about to descend the cooling branch (in the figure, shell-flash tracks are not explicitly shown but begin and end between the dotted lines). For those donors that evolve up the RGB, mass transfer stops when the donor turns off the RGB and the envelope collapses (Roche-lobe detachment). At this point the donor consists largely of a helium core ( $0.14 \lesssim (M_c/M_{\odot}) \lesssim 0.46$ ) on top of which resides a much less massive H-rich envelope ( $m_{env} \gtrsim 10^{-2}M_{\odot}$ ). The donor quickly evolves to the left on the HR diagram on a timescale of  $\sim 10^6$  to  $10^8$  years at approximately constant luminosity. Hydrogen burning continues and the value of  $m_{env}$  can be substantially reduced (by more than a factor of 2). After the maximum value of  $T_e$  is reached, there is a precipitous decrease in the luminosity and a sharp rise in the ratio of the ‘gravothermal luminosity’ to the nuclear luminosity (i.e.,  $L_g/L_{nuc}$ ). Further contraction of the envelope leads to (partial) adiabatic heating of the H-rich layer just above the He-core. Depending on the core mass and metallicity, the H-burning shell can either: (i) undergo a mild thermal readjustment (pulse); or, (ii) undergo a H-shell flash (unstable CNO burning). If the hydrogen re-ignites, the donor sometimes expands so much that it fills its Roche lobe causing further mass transfer (see, also, Sarna, Ergma, & Gerskevits-Antipova 2000, PRP). Eventually the thermonuclear runaway is quenched and the donor’s envelope collapses.

Figure 2 illustrates the temporal evolution of the luminosity for several initial core masses. For the  $1.5M_{\odot}$  case (left-hand panel),  $m_{c,o} = 0.00M_{\odot}$  produces a  $0.209M_{\odot}$  HeWD that experiences a thermal pulse but avoids unstable burning. The next three values of core mass,  $m_{c,o} = 0.05, 0.10, 0.15M_{\odot}$ , experience vigorous shell flashes. The last two cases corresponding to the highest values of  $m_{c,o}$  exhibit mild thermal pulses. The growth time of the burning instability and the thermal relaxation time of the envelope are comparable for these latter models and thus unstable burning is averted. The right-hand panel (initial  $1M_{\odot}$  donor) shows that the  $0.05M_{\odot}$  case is a good example of a multi-cyclic flash. For solar metallicities, we find that flashes are independent of the initial donor mass and occur for final HeWD masses in the range of  $0.21 \lesssim m_f/M_{\odot} \lesssim 0.28$ . These flashes can have a profound effect on the estimation of the ages of *young* pulsars based on the observed temperatures of the HeWDs. In fact, the cooling phase for HeWDs is quite different from that of C-O WDs in that H-burning

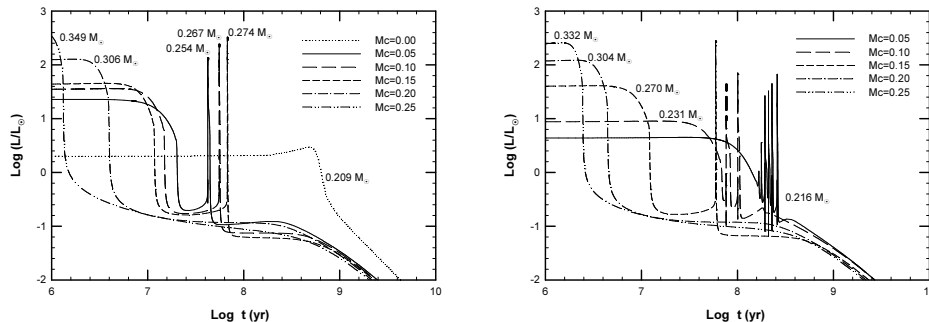


Figure 2. Temporal evolution of the luminosity of the donor ( $L$ ) as a function of the time elapsed since the cessation of mass transfer. For each curve on the left-hand panel, the initial mass of the donor is  $1.5M_{\odot}$  ( $Z = 0.02$ ) and the initial value of core mass ( $M_c$ ) at the onset of mass transfer is listed in solar units. The labels adjacent to each curve correspond to the final HeWD masses. The right-hand panel depicts the evolution of  $1.0M_{\odot}$  donors.

(via the pp-chain) can constitute an important fraction of the radiated energy for many billions of years.

Sample results of the evolution of  $P_{orb}$  with respect to the mass of the donor are shown in Figure 3 a). They too illustrate a sharp bifurcation in the evolution. Donors for which mass loss is very rapid evolve to smaller radii and  $P_{orbs}$ . The orbital period reaches a minimum value as the donor evolves towards the degenerate branch (and their radii increase). The  $X_c = 0.10$  case evolves to minimum period of  $\sim 35$  minutes (values as small as 8 minutes are possible [NR]). Examples of systems that may have evolved along this evolutionary pathway include the recently discovered ultracompact accreting millisecond X-ray pulsars: XTE J1751-305 (42.4 min), XTE J0929-314 (43.6 min), XTE J1814-338 (43.6 min), and XTE J1807-294 ( $\lesssim 40$  min). Donors above the bifurcation limit develop well-defined He cores, become larger in radius and evolve to higher periods. There is a strong correlation between the final period ( $P_{orb,f}$ ) and mass ( $m_f$ ) for specific metallicities. NDM have shown that for donors that develop well defined cores ( $m_f \gtrsim 0.25M_{\odot}$ ), the  $P_{orb} - m_f$  relation can be expressed as:

$$P_{orb,f} \simeq 2.5 Z^{0.3} 10^{10.7(m_f/M_{\odot})} \text{ hr} . \quad (1)$$

As noted by Ergma et al. (1998), donors that do not have well-developed cores at the onset of mass transfer will not obey a (universal)  $P_{orb} - m_f$  relationship. This issue is most clearly evident in systems that are near the bifurcation limit. The mode of angular momentum loss and assumptions concerning the accretion process can greatly affect the relationship. For example, the assumption of fully conservative mass transfer (i.e.,  $\beta = 1$ ) leads to different limits (see NDM).

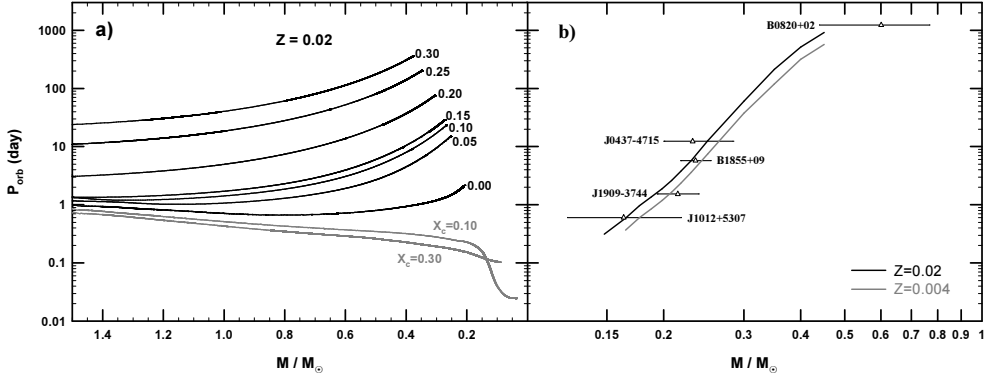


Figure 3. Panel a): Orbital period evolution of a donor whose initial mass is  $1.5M_{\odot}$  with a metallicity of  $Z = 0.02$ . The labels adjacent to each curve have the same connotations as those in Figure 1. A very sharp bifurcation is seen for initial values of  $P_{orb}$  of  $\lesssim 20$  hours. Panel b): The theoretically determined  $P_{orb} - M$  relationship for  $Z = 0.02$  is denoted by the solid black curve (the  $Z = 0.004$  case is denoted by the gray curve). The location of the “best-observed” companions are shown with their respective error bars (see van Kerkwijk 2004).

### 3.2. Cooling Evolution and Application to Observations

One of the most important and easily tested predictions of the theoretical models is the  $P_{orb} - m_f$  relationship. In Figure 3b the solid black curve shows the results for an extended grid of evolutionary models (it includes many new models near the bifurcation limit). Also shown are the most precisely determined observational data points including the respective error bars (see van Kerkwijk 2004). We see that good agreement is obtained for the majority of the observations. It is worth noting that B0820+02 has a period larger than the longest orbital period attainable from our models. It is quite likely that the donor in this system is actually a C-O WD (Koester & Reimers 2000). It should also be noted that J1909-38 is shifted to a higher mass value than would be expected based on the theoretical models. However, J1909-38 may have a lower metallicity than the solar value and this could explain its position in the diagram (see the  $Z = 0.004$  curve).

The models also tell us the cooling times of the HeWDs and thus the age of the pulsar after it has ‘turned on’. If these times can be established accurately then it may be possible to comment on the spin-down evolution of the pulsars by comparing the cooling times with the characteristic ages (see, e.g., Hansen & Phinney 1998). Assuming dipolar radiation and that  $P_o \ll P$ , the characteristic age can be approximated by  $\tau_{ch} = P/(2\dot{P})$ . Two particularly important systems are PSR J1012+5307 and PSR B1855+09. Using photometric techniques, van Kerkwijk, Bergeron, & Kulkarni (1996) determine the effective temperature of the HeWD in PSR J1012+5307 to be  $T_e = 8550 \pm 25\text{K}$  with an inferred  $\log g = 6.75 \pm 0.07$ . A later study by Callanan et al. (1998) allows for a much wider



range of values ( $T_e = 8670 \pm 300\text{K}$  and  $\log g = 6.31 \pm 0.2$ ). The characteristic age of the pulsar is  $\sim 7$  Gyr. Interpolating the NDM models (and assuming that  $T_e \simeq 8600\text{K}$ ) we conclude that the best fit for the companion corresponds to  $\log L/L_\odot = -2.1 \pm 0.2$ ,  $m_f = 0.17 - 0.18M_\odot$ ,  $t = 8 - 9$  Gyr, and  $\log g = 6.5 \pm 0.1$ . The cooling age for this donor (which does not undergo a flash and thus does not overflow its Roche lobe) is in very good agreement with the spin-down time inferred from the pulsar measurements. The importance of nuclear burning in these low-mass donors is also clearly demonstrated (Hansen & Phinney 1998 used much smaller envelope masses in their models and consequently found a cooling time of only  $\sim 0.5$  Gyr).

Although there is good agreement between the two timescales for PSR J1012+5307, the same cannot be said for PSR B1855+09. This BMSP is rather unique in that the mass of the companion has been measured quite precisely using the Shapiro delay (Kaspi, Taylor, & Ryba 1994). The mass is found to be  $\sim 0.258 \pm 0.02M_\odot$  and the characteristic age of the pulsar is thought to be  $\sim 5$  Gyr. The companion has been detected and its effective temperature is inferred to be  $4800 \pm 800\text{K}$  (van Kerkwijk et al. 2000). The relationship between  $P_{orb}$  and  $m_f$  is very good (see Figure 3b), but for a solar metallicity we find that a value of  $m_f \simeq 0.25M_\odot$  implies a cooling time of  $\gtrsim 10$  Gyr. While the result is not in unreasonable agreement with the characteristic age, the cooling time is approximately a Hubble time which seems to imply that the envelope is too thick to allow sufficient cooling. The recent theoretical models of Althaus, Serenelli, & Benvenuto (2001) that employed chemical diffusion seem to resolve this issue. They conclude that the HeWD can cool to the observed to within  $\sim 4$  Gyr. Diffusion may indeed be the answer but it is a very fragile physical process.

### 3.3. PSR J1740-5340

This unique eclipsing BMSP was discovered by D’Amico et al. (2001) in the globular cluster NGC 6397 and provides us with an excellent opportunity to test our theoretical understanding of the formation and evolution of BMSPs in clusters. Extensive photometry and spectroscopy have been carried out on this system and this has led to reasonably well-constrained values for the mass of the companion ( $\sim 0.3M_\odot$ ), its effective temperature ( $5410 \pm 50$  K), and luminosity ( $2.0 \pm 0.4L_\odot$ ) (see Orosz & van Kerkwijk 2003). The orbit is almost circular ( $e < 10^{-4}$ ) and the measured pulse period and characteristic age of the pulsar are 3.65 msec and  $\sim 350$  Myr, respectively. The cluster is extremely metal-poor,  $[\text{Fe}/\text{H}] = -2.0$ , and the MSP is located about 11 core radii from its center indicating that it probably underwent an exchange interaction. Because the position of the companion on the HR diagram is considerably to the red side of the cluster sequence, it has been classified as a ‘red straggler’.

In order to reproduce the observations, the evolution of  $0.8M_\odot$  donors having a metallicity appropriate to the cluster ( $Z = 0.0003$ ) has been calculated for a wide range of initial evolutionary states of the donor. This mass was chosen because a  $0.8M_\odot$  star in NGC 6397 is near TAMS (and just above the bifurcation limit). In order to obtain the best fit to the observations a mixing-length ratio of  $\alpha = l/H_p = 1$  was adopted (as opposed to 1.5 for the calculations described in the previous section). Also the assumed mode of angular momentum

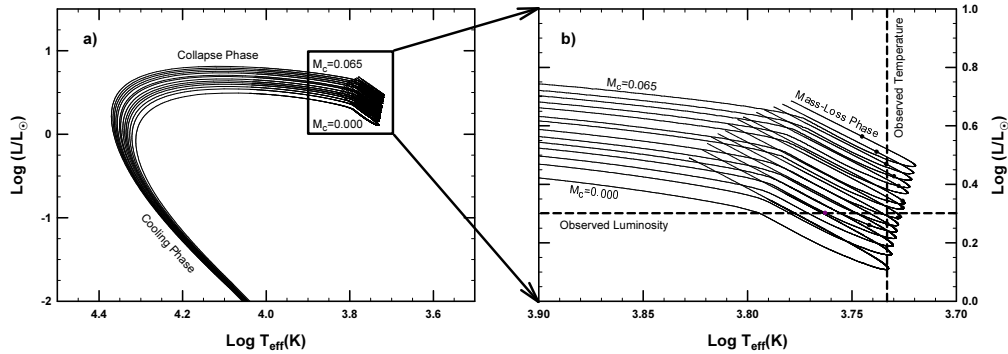


Figure 4. Panel a): Evolutionary tracks of donors with initial masses of  $0.8 M_{\odot}$  ( $Z = 0.0003$ ). The curve labeled  $M_c = 0.000$  corresponds to a donor whose initial He-core mass at the onset of mass transfer is  $0.00M_{\odot}$ . The interval between each track corresponds to a He-core mass difference of  $0.005 M_{\odot}$ . Note that mass loss starts at the beginning of each track (see panel b) and terminates at the beginning of the collapse phase (i.e., the approximately horizontal sections of each track). Panel b): Magnified view of the tracks. The observationally inferred values of  $L$  and  $T_{eff}$  of the donor are shown (dashed lines). The dots on each track correspond to the points where the orbital period matches the observed one (32.5 hours).

dissipation due to systemic mass loss is different. Although  $\beta$  is still zero (fully non-conservative mass loss), the specific angular momentum of the expelled matter is taken to be equal to that of the donor. Physically this assumption is consistent with a model wherein relativistic pulsar winds drive mass-loss uniformly from the donor’s surface. This scenario is similar to the ‘radioejection’ model described by Burderi, D’Antona, & Burgay (2002) in which they proposed that a temporary cessation of mass transfer would allow the pulsar to ‘turn on’ and that the radiation pressure at the inner Lagrange point would prevent further mass accretion by the pulsar (the matter is eventually ejected from the binary). According to this scenario the mass that is lost from the system carries away a specific angular momentum corresponding to the location of the Lagrange point (thus their models are, in general, less dissipative). It is assumed that the donor is approximately filling its Roche lobe as it loses mass. Both pictures could reasonably account for the type of eclipsing phenomena that is observed in PSR J1740-5340.

Figure 4 shows that the observed values of  $L$  and  $T_{eff}$  can be easily accommodated by the computed tracks. Based on the best fitting point from Figure 4 ( $P_{orb} = 32.5$  hr), it is likely that the mass of the donor is  $\sim 0.29 \pm 0.04M_{\odot}$  and that it is losing mass at a rate of  $\sim 5 \times 10^{-10}M_{\odot} \text{ yr}^{-1}$ . The inferred age of the donor after the cessation of accretion by the pulsar is  $\sim 0.5 \pm 0.1$  Gyr and this value is in good agreement with the spin-down age. In terms of detection probabilities, lower mass donors are strongly favored due to their slower evolution. The only requirement is that the donor be reasonably well evolved (e.g., near

TAMS) at the onset of mass transfer. In fact, the detection of a BMSP system with these observed properties is *relatively* likely (assuming that the pulsar does turn on and radioejection is possible) since the derivative,  $dT_{eff}/dt$ , is reasonably flat ( $T_{eff}$  remains within a range of  $\pm 100\text{K}$  for  $\gtrsim 200$  Myr). Finally it is very important to note that if the binary were to experience another dynamical encounter in which the donor (i.e., straggler) were to be ejected, then it would likely remain classified as single ‘red straggler’ for a substantial fraction of time (on the order of a Gyr) before evolving back to a point close to the cluster’s HR-sequence.

#### 4. Conclusion

While the theoretical models have been successful in explaining many of the observational details, there are still some important open questions and apparent inconsistencies that need to be addressed. Specifically, these include: (i) How much mass does the neutron star accrete while it is being spun up to msec periods? (ii) What fraction of BMSPs can trace their lineage from the evolution of intermediate-mass X-ray binaries? (iii) What is the nature of the discrepancy between the birthrates for X-ray binaries and BMSPs? (iv) How important a role does irradiation play in affecting the evolution of the progenitor systems? (v) What is the importance of diffusion in determining the cooling times of the degenerate companions? (vi) How were the very-short orbital period ( $< 1$  day) systems formed? These are questions that can be investigated individually, but only a robust population synthesis that reproduces all of the salient observations will allow us to conclude that the issues have been resolved.

**Acknowledgments.** This research was supported in part by a grant from the Canada Research Chairs program and NSERC (Canada). I would like to acknowledge the technical assistance of E. Dubeau, J. Benjamin and the Centre de Calcul Scientifique (Université de Sherbrooke). I am also indebted to S. Rappaport and M. van Kerkwijk for numerous insightful discussions.

#### References

- Althaus, L.G., Serenelli, A.M., & Benvenuto, O.G. 2001, MNRAS, 324, 617  
 Backer, D. C., Kulkarni, S. R., Heiles, C., Davis, M. M., & Goss, W. M. 1982, Nature, 300, 615  
 Bhattacharya, D. & van den Heuvel, E.P.J. 1991, Phys. Rep., 203, 1  
 Bitzaraki, O.M., van den Heuvel, E.P.J., Tout, C.A., & Rovithis-Livaniou, H. 2003, in ASP Conf. Ser. 302, Radio Pulsars, ed. M. Bailes, D. Nice & S. Thorsett (San Fransisco: ASP), 313  
 Burderi, L., D’Antona, F., & Burgay, M. 2002, ApJ, 574, 325  
 D’Amico, N., Lyne, A.G., Manchester, R.N., Possenti, A., & Camilo, F. 2001, ApJ, 548, L171  
 Ergma, E., Sarna, M.J., & Antipova, J. 1998, MNRAS, 300, 352  
 Hansen, B.M.S. & Phinney, E.S. 1998, MNRAS, 294, 569  
 Howell, S. B., Nelson, L. A., & Rappaport, S. 2001, ApJ, 550, 897

- Kaspi, V.M., Taylor, J.H., & Ryba, M.F. 1994, *ApJ*, 428, 713
- Koester, D. & Reimers, D. 2000, *A&A*, 364, L66
- Nelson, L.A. & Dubeau, E. 2004, (in preparation)
- Nelson, L.A., Dubeau, E., & MacCannell, K. 2004, *ApJ*, (in press) [NDM]
- Nelson, L.A. & Rappaport, S. 2003, *ApJ*, 598, 431 [NR]
- Nice, D., Splaver, E.M., & Stairs, I.H. 2003, in *ASP Conf. Ser.* 302, *Radio Pulsars*, ed. M. Bailes, D. Nice & S. Thorsett (San Fransisco: ASP), 313
- Orosz, J.A. & van Kerkwijk, M.H. 2003, *A&A*, 397, 237
- Pfahl, E.D., Rappaport, S., & Podsiadlowski, Ph. 2003, *ApJ*, 597, 1036
- Phinney, E.S. & Kulkarni, S.R. 1994, *ARA&A*, 32, 591
- Podsiadlowski, Ph., Rappaport, S., & Pfahl, E.D. 2002, *ApJ*, 565, 1107 [PRP]
- Pylyser, E. & Savonije, G.J. 1988, *A&A*, 191, 57
- Rappaport S., Podsiadlowski Ph., Joss P.C., Di Stefano R., & Han Z. 1995, *MNRAS*, 273, 731
- Rappaport, S., Verbunt, F., & Joss, P. C. 1983, *ApJ*, 275, 713
- Sarna, M.J., Ergma, E., & Gerskevits-Antipova, J. 2000, *MNRAS*, 316, 84
- Taam, R.E., King, A.R., & Ritter, H. 2000, *ApJ*, 541, 329
- Tauris, T.M. & Savonije, G.J. 1999, *A&A*, 350, 928
- Tauris, T.M., van den Heuvel, E.P.J., & Savonije, G.J. 2000, *ApJ*, 530, L93
- van Kerkwijk, M.H. 2004, in *ASP Conf. Ser.*, *Binary Radio Pulsars*, ed. F. Rasio & I. Stairs (in press)
- van Kerkwijk, M.H., Bell, J.F., Kaspi, V.M., & Kulkarni, S.R. 2000, *ApJ*, 530, L37
- van Kerkwijk, M.H., Bergeron, P., & Kulkarni, S.R. 1996, *ApJ*, 467, L89
- van Straten, W., Bailes, M., Britton, M., Kulkarni, S.R., Anderson, S.B., Manchester, R.N., & Sarkissian, J. 2001, *Nature*, 412, 158
- Wijnands, R. & van der Klis, M. 1998, *ApJ*, 507, L63
- Willems, B. & Kolb, U. 2002, *MNRAS*, 337, 1004